Volume 16 | Number 2 | 21 January 2016 | Pages 219–390

Lab on a Chip

Miniaturisation for chemistry, physics, biology, materials science and bioengineering

www.rsc.org/loc

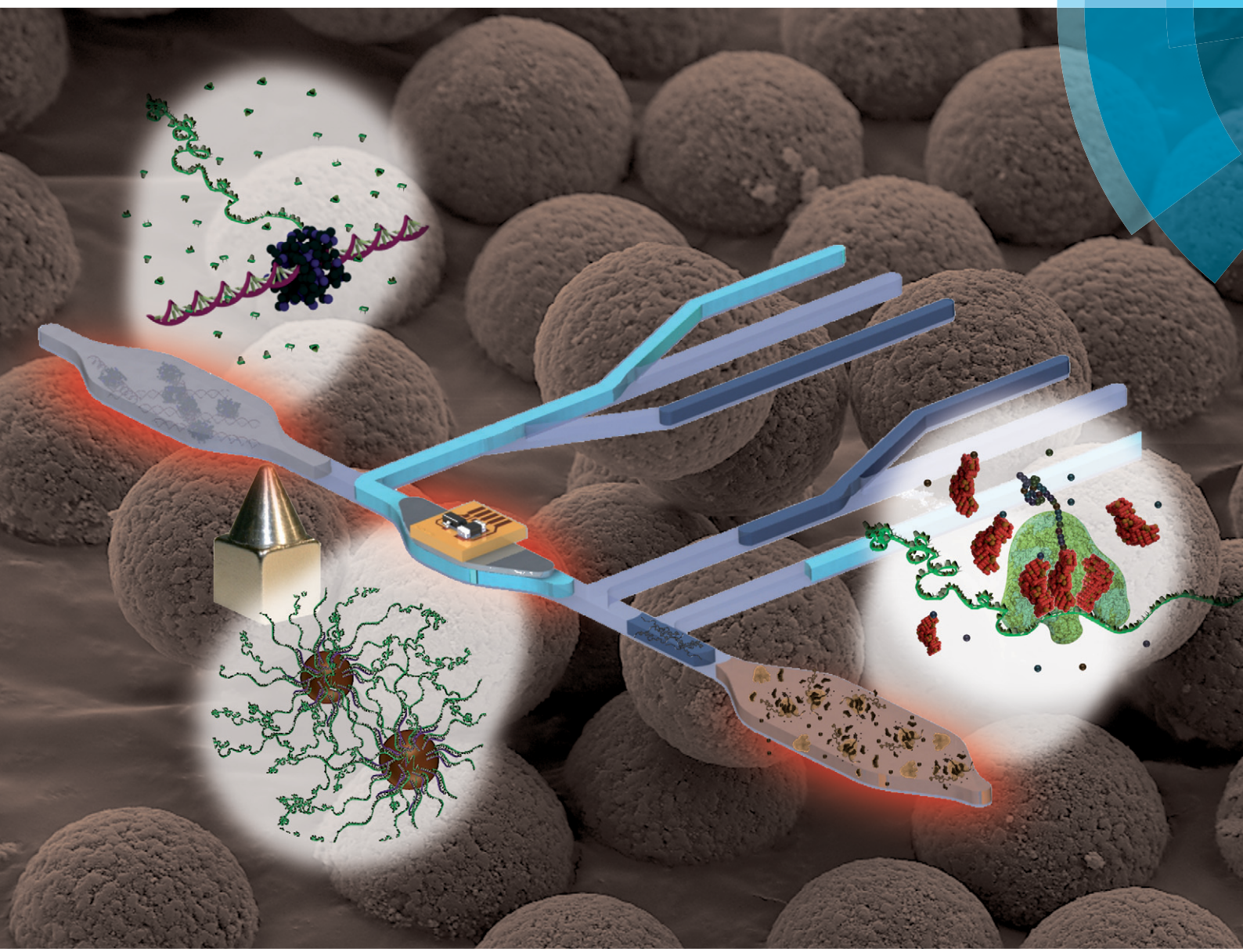

ISSN 1473-0197

ROYAL SOCIETY OF CHEMISTRY

PAPER
Stefan Kubick *et al.*
On-chip automation of cell-free protein synthesis: new opportunities due to a novel reaction mode

175 YEARS

Lab on a Chip

PAPER

View Article Online
View Journal | View Issue

Cite this: *Lab Chip*, 2016, **16**, 269

On-chip automation of cell-free protein synthesis: new opportunities due to a novel reaction mode†

V. Georgi,[ab] L. Georgi,[c] M. Blechert,[a] M. Bergmeister,[a] M. Zwanzig,[c] D. A. Wüstenhagen,[b] F. F. Bier,[b] E. Jung[a] and S. Kubick*[b]

Received 22nd June 2015,
Accepted 22nd October 2015

DOI: 10.1039/c5lc00700c

www.rsc.org/loc

Many pharmaceuticals are proteins or their development is based on proteins. Cell-free protein synthesis (CFPS) is an innovative alternative to conventional cell based systems which enables the production of proteins with complex and even new characteristics. However, the short lifetime, low protein production and expensive reagent costs are still limitations of CFPS. Novel automated microfluidic systems might allow continuous, controllable and resource conserving CFPS. The presented microfluidic TRITT platform (TRITT for Transcription – RNA Immobilization & Transfer – Translation) addresses the individual biochemical requirements of the transcription and the translation step of CFPS in separate compartments, and combines the reaction steps by quasi-continuous transfer of RNA templates to enable automated CFPS. In detail, specific RNA templates with 5′ and 3′ hairpin structures for stabilization against nucleases were immobilized during *in vitro* transcription by newly designed and optimized hybridization oligonucleotides coupled to magnetizable particles. Transcription compatibility and reusability for immobilization of these functionalized particles was successfully proven. mRNA transfer was realized on-chip by magnetic actuated particle transfer, RNA elution and fluid flow to the *in vitro* translation compartment. The applicability of the microfluidic TRITT platform for the production of the cytotoxic protein Pierisin with simultaneous incorporation of a non-canonical amino acid for fluorescence labeling was demonstrated. The new reaction mode (TRITT mode) is a modified linked mode that fulfills the precondition for an automated modular reactor system. By continual transfer of new mRNA, the novel procedure overcomes problems caused by nuclease digestion and hydrolysis of mRNA during TL in standard CFPS reactions.

Introduction

In recent years, cell-free protein synthesis (CFPS) evolved into a promising alternative to cell-based protein expression systems.[1–4] CFPS is based on cell extracts – the required cellular tools are applied for *in vitro* protein synthesis. The absence of cell walls leads to an open system allowing continuous monitoring and specific adaptation of the reaction parameters. Additionally the introduction of non-canonical amino acids enables production of proteins with completely new biochemical properties.[5–8] Moreover, many metabolites and protein products are toxic to living cells or induce toxic effects in higher concentrations. For instance, the expression of the pharmacologically relevant membrane proteins causes severe problems *in vivo*, such as toxic effects due to system overload by transport and pore forming activities and membrane destabilization.[9] However, membrane proteins,[10–16] cytotoxic proteins[17,18] and further "otherwise difficult-to-express" proteins can be produced efficiently with cell-free systems. In summary, CFPS has enormous potential for pharmacological applications,[19–23] protein evolution[24] and structural and functional proteomics.[25]

The whole process of CFPS was optimized in the past – especially at the biochemical level – in terms of higher yields and functional protein activity,[26–28] but also special reaction modes and formats were developed. In general, CFPS is nowadays performed in two ways: 1) the coupled system: transcription (TK) and translation (TL) are performed simultaneously in the same reaction compartment, or 2) the linked system: TK and TL are performed consecutively and are separated physically. The linked system enables optimal adaption of the reaction conditions for TK and TL and optimal yields

[a] *Fraunhofer Institute for Reliability Microintegration, Department System Integration & Interconnection Technologies, Working Group Medical Microsystems, Berlin, Germany. E-mail: Erik.Jung@IZM.Fraunhofer.de; Fax: +49 (0)30/464 03 161; Tel: +49 (0)30/464 03 230*
[b] *Fraunhofer Institute for Cell Therapy and Immunology (IZI), Branch Bioanalytics and Bioprocesses Potsdam-Golm (IZI-BB), Potsdam, Germany. E-mail: stefan.kubick@izi-bb.fraunhofer.de; Fax: +49 (0)331/581 87 399; Tel: +49 (0)331/581 87 306*
[c] *Technische Universität Berlin, Faculty Electrical Engineering Computer Science, Microperipheric Technologies, Berlin, Germany*

† Electronic supplementary information (ESI) available: See DOI: 10.1039/c5lc00700c

of active proteins. Furthermore there are different formats for *in vitro* translation. The simplest format is the batch reaction, where all components are simultaneously combined in one reaction vessel. As an alternative there are other formats: the continuous flow cell-free translation system and a simpler dialysis version – the continuous exchange cell-free system. Both allow longer reaction times, and thus higher yields, due to the permanent removal of low-molecular weight by-products inhibiting the reaction and a permanent feeding with substrate and energy sources.[29–32] However, short reaction times, low protein yields and high reagents costs remain limitations of CFPS. The short lifetime of mRNA is caused by hydrolysis and nuclease digestion and is still a drawback of CFPS. Translation of immobilized mRNA was previously performed to stabilize the labile RNA against nucleases, but this method resulted in much lower protein yields compared to TL of free mRNA.[33,34]

Novel automated modular microfluidic systems with integrated sensors for online monitoring and regulation of relevant process parameters could allow a continuous, controlled and resource-conserving CFPS. The presented microfluidic TRITT platform fulfills the precondition for such a modular micro-reactor: the active transfer of the product of transcription (RNA) from the TK to a separate TL compartment, where the RNA serves as template for protein synthesis, is realized in an automatable manner. In this way the TRITT platform allows a novel reaction mode – called TRITT mode for "Transcription – RNA Immobilization & Transfer – Translation" (Fig. 1). Since TK and TL are performed in separate reaction compartments, the biochemical requirements can be addressed individually. Thus the new reaction mode is similar to the linked mode, but in the TRITT mode TK and TL can be performed at the same time and transcription is not inhibited or terminated by RNA transfer. Furthermore the transfer of RNA can be started right at the beginning of transcription, which is time saving. The TRITT concept should be compatible with all reaction formats described above. For instance a combination of the presented TRITT platform with the dialysis format for translation would allow renewal of energy and substrates and removal of by-products by dialysis and simultaneously optimal conditions for TK and TL as well as feeding with new RNA, both enabled by the TRITT mode. This combination would lead to longer reaction times under optimal conditions.

To our knowledge the novel TRITT mode enables for the first time automated CFPS in a modular reactor with continuously optimal synthesis conditions simultaneously for the reaction steps TK and TL. Moreover, the quasi-continuous transfer of RNA to the TL compartment compensates the problem of RNA degradation and hydrolysis.

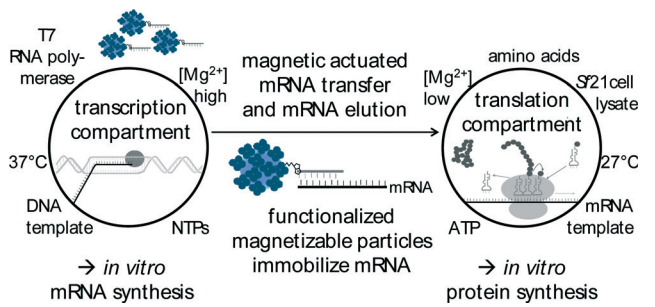

Fig. 1 Principle of the microfluidic TRITT platform. The TRITT platform enables operation of the cell-free system in the novel TRITT mode (= Transcription – RNA Immobilization & Transfer – Translation). Due to quasi-continuous mRNA transfer, there are continuous optimal synthesis conditions simultaneously for TK and TL.

Materials and methods

Device design and fabrication

Fig. 2 gives an overview of the microfluidic device for cell free protein synthesis. The microfluidic pattern (Fig. 2A and B; Fig. S1†) was micro-milled into 1.55 mm high amorphous thermoplastic Cyclic Olefin Copolymer COC (TOPAS 6013-S04) substrate using the Datron M7 milling machine with 0.3–1 mm cutters. Drilled access holes enabled fluid connection. To form a fluid-tight microfluidic device with homogenous surface properties, the patterned substrate with the rectangular channels (500 μm wide and deep), reaction chambers (height 500 μm; area of TK chambers: 29.5 mm^2, of elution chamber: 8 mm^2, of TL chambers: 59.4 mm^2) and access holes was permanently bonded to a 135 μm thick COC foil (TOPAS 6013) as cover plate (Fig. 2A) by thermal bonding technique. In detail, thermal bonding was performed at 138 °C and 2–5 kN using a modified vacuum wafer bonder AML AWB-04. Steel cannulas were glued into access holes, and silicone tubing was slipped over the cannula for fluid connection. Fluid actuation was finally realized by pressure differences caused by syringe pumps. Other access holes served as filling ports for fluid application with a pipet tip. The micro-milled microfluidic COC walls were modified by a coating with a low-viscosity solution with a fluoro-acrylate-polymer dissolved in the organic solvent hydrofluoroether (Certonal FC-742, Nordson Deutschland GmbH). Flushing with the dissolved fluoro-acrylate-polymer leads to deposition of a dry, transparent, oleophobic and hydrophobic film adhering to the microfluidic walls through intermolecular interactions and modifying surface properties such as roughness, surface tension and surface charge. Process temperatures were controlled by integrated thermal sensors (PT1000 or Microchip TC1047A) and actuators, such as heating pads (RS 245-499; 12 V, 1.25 W) and thermal resistors (1206 100R; 2 in parallel), mounted on heat spreaders of aluminum (Fig. 2A and C). Three temperature zones are realized on the chip: 37 °C for transcription chambers, 70 °C for the elution chamber and 27 °C for the translation chamber (Fig. 2B). Homogeneity of the heating over the surface was verified by IR thermography (IR-Cam SC6000). Air slots were drilled around the elution chamber to ensure proper heat insulation between the different temperature zones (verified by IR thermography). For the manipulation of the RNA transferring magnetizable particles in the microfluidic platform, a permanent magnet with a

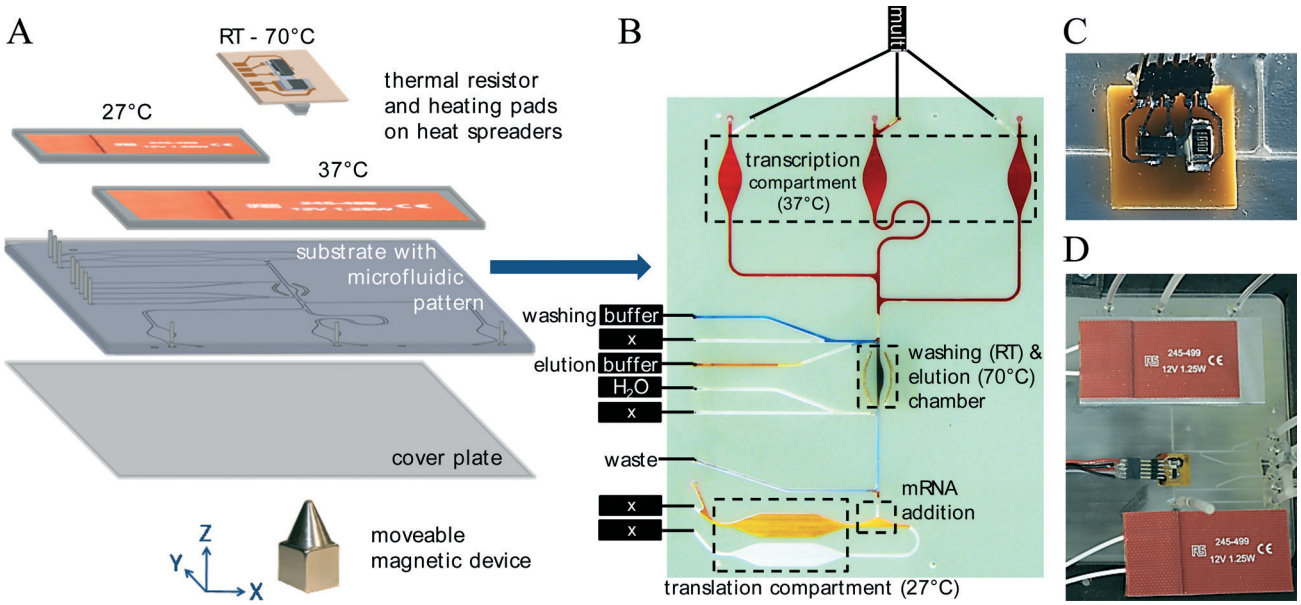

Fig. 2 Overview of the microfluidic TRITT platform for CFPS. (A) Exploded view of chip composition. A COC substrate with the microfluidic patterns was permanently bonded to a COC cover plate by thermal bonding technique. Thermal sensors and actuators mounted on heat spreaders and attached to the microfluidic chip controlled process temperatures. A movable magnetic device transferred magnetizable particles and bound mRNA in the microfluidic structures. (B) Bottom view of the microfluidic device. The microchannels are highlighted by different fluid dyes. TK compartment is divided into three chambers for successive immobilization of the synthesized mRNA to functionalized magnetizable particles. Following transfer of the mRNA loaded particles, the particles were washed for complete removal of the TK mixture, and mRNA was removed by temperature and low salt driven elution. The mRNA containing solution was mixed with the translation mixture where the mRNA serves as template for protein synthesis. The particles were reused for immobilization. (C) Integrated thermal resistor and sensor for temperature control. A PCB assembled with a thermal resistor and a temperature sensor was mounted on a heat spreader and attached to the microfluidic compartment with thermally conductive paste. (D) Photograph of the microfluidic system (top view). The TRITT chip is placed upon an apparatus for magnet movement (motorized *xyz*-positioning system; Fig. S2†). Magnetizable particles in the microfluidic structure follow the magnetic field.

cone-shaped add-on piece (Fig. 2A) was mechanically moved using a motorized *x*–*y*(–*z*) stage. The add-on piece was required to focus the magnetic field of a 10 mm^3 cubical NdFeB permanent magnet (Br – 13 000 gauss). To design the geometry of the magnetic device, the magnetic flux density around the device was calculated using the finite element method (FEM) software ANSYS (version 14.5).

Device operation

After rinsing the microfluidic structures with DEPC (diethylpyrocarbonate) treated water, the chip was placed upon an apparatus for magnet movement – the motorized *xyz*-positioning system (Fig. S2†) with the magnetic device tip less than 1 mm underneath the thin cover plate of the microfluidic chip. The thermal actuators (1206 100R or RS 245-499) were connected to their driving circuit of a microcontroller operated control unit, which was designed and fabricated in-house: temperatures were feedback-controlled using the integrated sensors (PT1000 or Microchip TC1047A). The syringes were attached to the channels with the tubing. All syringes were actuated using a syringe pump array developed in-house that was controlled by a LabVIEW program. The buffers and solutions were filled in the compartments of the chip with the syringe pumps or a pipette tip, and the filling ports were closed.

The microfluidic TRITT platform for Transcription – RNA Immobilization & Transfer – Translation works as follows: functionalized magnetizable particles immobilize the mRNA synthesized in the TK compartment. In the first run, the TK mixture was pumped and the particles of the first TK chamber were transferred to the washing and elution chamber. The TK mixture was pumped back to the TK compartment and the particles were conditioned using washing buffer. Washing removes residuals of the TK mixture and prepares the particles for elution. mRNA was removed by temperature (70 °C) and low salt driven elution. The mRNA was pumped to the TL compartment and mixed with the TL mixture. During the transfer process, the temperature of the mRNA containing eluate dropped to RT avoiding denaturation in the TL mixture. Finally the particles were transferred back to the first TK chamber. In the following runs, the same procedure was repeated with the particles in the second and the third TK chamber and the first chamber again and so on. During transfer of the particles of the other chambers, mRNA is again immobilized to the particles in the resting chamber.

The precise chip operation is illustrated in Fig. S3.†

Generation of DNA templates for *in vitro* TK

Linear DNA templates were generated by two-step Expression PCR (E-PCR)[35] using the Easy Express Linear Template Kit

PLUS (Qiagen) according to the manufacturer's instructions. Theoretical product sizes were calculated in silico, and the PCR products were analyzed by gel electrophoresis. The bands of the products appeared at their expected sizes (data not shown).

For generation of eYFP and Pierisin templates suitable for *in vitro* TK, the coding sequences of eYFP and Pierisin were amplified in the first PCR step by using eYFP-specific primers x-eXFP-F and x-eXFP-R and the Pierisin-specific primers x-Pierisin-F and x-Pierisin-R (all primer sequences are listed in Table 1). In the second PCR step the adapter primer no taq sense primer and no taq antisense primer were used to add regulatory elements for cell-free protein synthesis as well as a specific hairpin structure for stabilization against ribonucleases to the eYFP gene and the Pierisin gene.

For fusion of eYFP with the appropriate IRES elements, the coding sequence of eYFP and the IRES sequences were amplified separately in the first PCR step: eYFP was amplified by using the gene-specific primers eYFP-F (ATg gTg AgC AAg ggC gAg gAg) and x-eXFP-R. IRES elements were amplified by using the primers x-KSHV252-F and either R-KSHV252(+s)-oe-eYFP or R-KSHV252(−s)-oe-eYFP. In the second PCR step the genes were fused to each other and the adapter primers no taq sense primer and no taq antisense primer harboring the previously described functional elements were added.

Alternatively, DNA templates were linearized by EcoRI restriction nuclease treatment of the vector pIX3.0-eYFP or pIX3.0-Luc.

Preparation of standard insect cell lysates

CFPS was performed in translationally active lysates derived from cultured *Spodoptera frugiperda* (*Sf21*) cells. The *Sf21* cells were grown in fermenters in a chemically defined, serum-free medium under well-controlled conditions for optimal cell-growth: temperature (27 °C), air flow, oxygen, carbon dioxide and cell density were permanently controlled. At a cell density of approximately 5×10^6 cells per mL the *Sf21* cells were collected by centrifugation and translationally active lysates were prepared as previously described by Sachse *et al.*[36]

Cell-free protein synthesis

The cell-free system was operated in the linked transcription-translation mode and in the novel modified linked mode (TRITT mode), respectively. In the linked mode, TK and TL are performed successively and were separated physically by an mRNA purification step.[13] In the TRITT mode, TK and TL are also performed in two compartments but at the same time, and mRNA is continually transferred to the TL compartment using functionalized particles.

In this study the linked procedure was performed manually in standard reaction vessels using thermo mixers (comfort, Eppendorf) for temperature control. mRNA synthesized during *in vitro* TK was purified immediately following TK. Therefore, DyeEx spin columns (Qiagen) and alternatively functionalized magnetizable particles were used for mRNA purification prior to *in vitro* TL. In contrast, a microfluidic device was developed to enable solely the novel TRITT mode. The microfluidic TRITT platform controls the process temperatures by integrated thermal sensors and actuators. The continual mRNA transfer is realized by immobilization of mRNA to magnetizable particles during TK and software-controlled magnetic actuated particle transfer and fluid flow to the TL compartment.

The same reaction mixtures were used for both modes of transcription-translation procedure. *In vitro* TK was performed as described previously[17] using T7 polymerase (polymerase and buffer from Agilent, nucleoside triphosphates from Roche). The mixture was incubated for 2–19 h at 37 °C. For *in vitro* TL, the translationally active *Sf21* cell lysate (40% v/v) containing ribosomes, soluble enzymes, tRNAs and translation initiation and elongation factors was supplemented with mRNA (>200 ng μL^{-1}), canonical amino acids (200 μM), energy sources (1.75 mM ATP, 0.45 GTP) and an energy regenerating system (20 mM creatine phosphate and 100 μg mL^{-1} creatine kinase). For protein labeling and quality control by incorporation of non-canonical amino

Table 1 Primer sequences for template generation by expression PCR

Primer	Sequence (5′→3′)
x-eXFP-F	AgA Agg AgA TAA ACA ATg gTg AgC AAg ggC gAg gAg C
x-eXFP-R	CTT ggT TAg TTA gTT ATT ACT ACT TgT ACA gCT CgT CCA TgC Cg
x-Pierisin-F	AgA Agg AgA TAA ACA ATg TCT AAC AAT CCA CCC TAC ATg ACT A
x-Pierisin-R	CTT ggT TAg TTA gTT ATT ACA TTA gAA TAA AAT gAA ATA ATT gAT TAT CCg AAT
No taq sense primer	ATg ATA TCT CgA gCg gCC gCT AgC TAA TAC gAC TCA CTA Tag ggA gAC CAC AAC ggT TTC CCT CTA gAA ATA ATT TTg TTT AAC TTT AAg AAg gAg ATA AAC AAT g
No taq antisense primer	ATg ATA TCA CCg gTg AAT TCg gAT CCA AAA AAC CCC TCA AgA CCC gTT TAg Agg CCC CAA ggg gTA CAg ATC TTg gTT AgT TAg TTA TTA
eYFP-F	ATg gTg AgC AAg ggC gAg gAg
x-KSHV252-F	TTA AgA Agg AgA TAA ACA gTg CgC TgT Tgg TTC CTg
R-KSHV252 (+s)-oe-eYFP	CTC gCC CTT gCT CAC CAT TTg gAT CAT TCg CCC TTT Tg
R-KSHV252 (−s)-oe-eYFP	CTC gCC CTT gCT CAC CAT ggT gCC ggC TTg TAT ATg

acids, ^{14}C-labeled leucine (GE Healthcare) and Bodipy-TMR-lysine (from RiNA GmbH; 2 μM final concentration) were added to the reaction mixtures. The mixture was incubated for 1.5 h or 2 h at 27 °C.

Determination of RNA and protein yields and quality control

The yield and purity of *in vitro* transcribed mRNA was analyzed spectrometrically (NanoDrop 2000c or SpectroStar Nano) prior to mRNA application for immobilization or *in vitro* translation. The mRNA was additionally analyzed by agarose gel electrophoresis. All products were detected as homogenous bands showing the expected size (data not shown).

The amount of active *in vitro* translated eYFP was quantified by fluorescence analysis. Samples were diluted 1 : 5 in phosphate buffered saline (PBS without Mg^{2+} and Ca^{2+}, Biochrom AG), transferred to 18 well μ-slides (from Ibidi), and eYFP fluorescence was determined using a fluorescence scanner (Typhoon Trio + Imager, GE Healthcare) with an excitation wavelength of 488 nm. The analysis software "ImageQuant TL" was used for relative quantification of eYFP by comparison of the arbitrary fluorescence units in the digitalized images.

SDS-PAGE migration of *de novo* synthesized proteins was analyzed by subjecting 5 μL samples of the translation mixture to cold acetone precipitation. Precipitated proteins were resuspended in 20 μL sample buffer (NuPAGE® LDS Sample Buffer, Invitrogen) and loaded on pre-casted NuPAGE® 10% Bis-Tris polyacrylamide gels (Invitrogen). Separation was performed at 180 V for approximately 45 min. Finally the labeled proteins were visualized using the Typhoon Trio + Imager System (GE Healthcare).

Functionalization of magnetic particles and elution of RNA

Newly designed biotinylated hybridization oligonucleotides (HybOligos) were coupled to streptavidin-coated particles (Dynabeads® MyOneTM Streptavidin C1, Invitrogen) according to the manufacturer's instructions. Four different HybOligos were designed: Hyb3A (Biotin – 5′ ggT ACA gAT CTT ggT TAg TTA gTT A 3′) and Hyb3B (Biotin – 5′ CAA AAA ACC CCT CAA gAC CCg TTT A 3′) binding to the 3′ untranslated region (UTR) of the RNA template, as well as Hyb5A (5′ AAA gTT AAA CAA AAT TAT TTC TAg A 3′ – Biotin) and Hyb5B (5′ ATT ATT TCT AgA ggg AAA CCg TTg T 3′ – Biotin) binding to the 5′UTR of the RNA template. Additionally, Hyb3A and Hyb5A were flanked by an oligo$(dT)_{15}$ spacer at their site of biotinylation to enhance the distance between the magnetizable particle and the site of hybridization. RNA Immobilization to functionalized magnetic particles was evaluated applying a number of different conditions (incubation temperatures and times, HybOligos). Various particles (Dynabeads® Streptavidin Trial Kit, Invitrogen) were analyzed for applicability in the microfluidic TRITT platform.

RNA loaded particles were washed: different washing solutions (low salt buffers), volumes, times and repetitions of washing were tested. Elution was performed at 70 °C for 2 min using different elution solutions (water or low salt buffers). Elution leads to denaturation of the hydrogen bonds formed between the HybOligo and the RNA template, releasing the RNA from the particles, but the procedure cannot disrupt the interaction between streptavidin and biotin. The midpoint temperature of thermally induced denaturation of streptavidin is dependent on the saturation with biotin and ranges from 75 °C to 112 °C.[37] At least one binding site of streptavidin is occupied with a Biotin-HybOligo. Thus the HybOligos were not removed from the particles by the elution procedure. This was additionally experimentally verified (data not shown).

Results and discussion

Design of the magnetic device for separation and transfer of the magnetizable particles and bound molecules

The core of a modular reactor system is a linkage of the reaction compartments by transfer of the intermediates. The TRITT platform presented here allows transfer of the productof transcription (mRNA) from the transcription to the translation compartment where it serves as template for protein synthesis. This mRNA transfer is realized by magnetizable particles. A special functionalization allows immobilization of the mRNA. Particle separation and transfer is realized by movement of an external permanent magnet. The permanent magnet is moved by a *xyz*-positioning system (Fig. S2†). The *z*-lifting enables the combination of the strong volumetric magnetic fields and forces of permanent magnets with the ability to vary the magnetic forces on the particles in the microfluidic structure. Furthermore, the magnetic field was focused with the help of a cone-shaped add-on piece allowing the application of a large permanent magnet with a high magnetic adhesive force and simultaneous focused field lines resulting in a small particle cluster. The magnetic flux densities around the magnetic devices were simulated using a commercial Finite-Element-Method-Software (3D simulation in Fig. 3A). The cover plate sealing the microfluidic patterns is thin to decrease the distance to the magnet and thereby enhance the local magnetic field gradient. Fig. 3B shows different particle configurations corresponding to different positions of the magnetic device. As seen in the left picture of the microfluidic washing and elution compartment (Fig. 3B), the particles can be captured at the wall facilitating fluid exchange. Moreover, by adjustment of the distance between the magnetic device and the particles (*z*-lifting), the particles in a microfluidic chamber can either be collected in a small cluster for transfer (approx. 700 μm) or can be dispersed for immobilization (approx. 2 cm) (Fig. 3B).

Surface modification of the microfluidic structures for manipulation of wettability and interaction with particles

On the one hand the magnetic actuated transfer of the magnetizable particles requires liquid media. On the other hand the diffusion between the individual reaction mixtures and

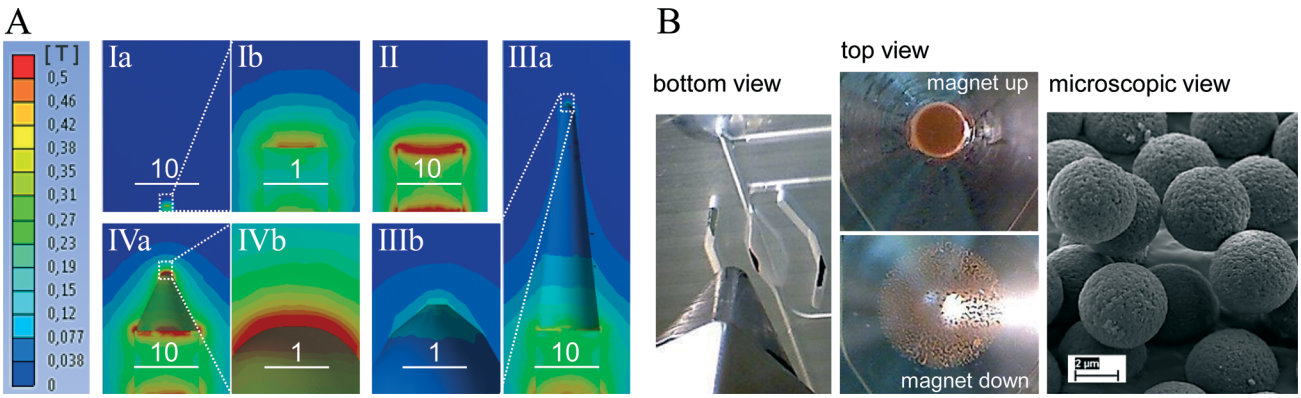

Fig. 3 Magnetic device for manipulation of magnetizable particles. (A) 3D FEM Simulations of the magnetic flux density in air around a 1 mm^3 cubical permanent magnet (I) and a 1 cm^3 cubical permanent magnet with (III, IV) and without (II) cone-shaped add-on pieces (scale bars in mm; solid bodies hidden; flux density in tesla). Due to its low magnetic adhesive force (≈0.363 N) the 1 mm^3 permanent magnet was not able to collect all the suspended particles in the TK chamber. The 1 cm^3 magnet itself has a higher magnetic adhesive force (≈37.3 N) but its magnetic field has to be focused with the help of an add-on piece. The length of the add-on piece influences the magnetic flux density around its tip. The add-on piece IV was used in the presented microfluidic TRITT platform since it possesses a high magnetic flux density on a small area (≈1 × 1 mm^2). The calculated magnetic flux density approximately 700 µm above the tip is ≈0.3 T. (B) The magnetic device allows manipulation of the magnetizable particles. As seen in the photographs of the particles (brown) in the microfluidic structures, different particle configurations can be achieved by movement of the magnetic device. The add-on piece allows formation of a small particle cluster for transfer as well as fixation of particles at the channel's wall enabling fluid exchange. Alteration of the distance between the particles and the magnetic device leads to dispersed (approx. 2 cm) and aggregated particles (approx. 700 µm), respectively. An electron micrograph of magnetizable particles is depicted on the right hand side.

solutions has to be limited. Various liquid separation media such as tetradecane were tested, but were incompatible with the cell-free reactions or the immobilization procedure (data not shown). Therefore air was used as separation medium, and particle transfer was realized as follows: the particles were transferred in a liquid medium (for instance TK mixture), the liquid was then drawn back, and the particles were resuspended in the new solution (for instance washing buffer). However, repeated pumping in the micro-milled microfluidic COC structures led to uncontrolled flow behavior and incomplete filling of microfluidic chambers (Fig. 4B). Trapped air bubbles arose and hindered magnetic actuated particle transfer. Furthermore particles adhered to the COC surface (Fig. 4C). Accordingly, the surface properties – surface charge, roughness and surface tension – of the microfluidic walls were changed to manipulate wettability and the interaction with particles. In detail, the micro-milled COC surface was modified by a coating with a fluoro-acrylate-polymer. Fluoro-acrylate-polymers are usually applied in electronics and are here effectively applied in the new field of microfluidics. Fluoro-acrylate-polymer coating leads to a more hydrophobic surface (Fig. 4A) and allows pumping with repeated defined fluid flow (Fig. 4B). Additionally, the adherence of the particles to the microfluidic surface is decreased by the fluoro-acrylate-polymer coating (Fig. 4C).

Design and optimization of mRNA immobilization

The special RNA template without polyA tail, which is stabilized against ribonuclease digestion by optimized hairpin structures at the 3′ and 5′ end, has to be immobilized to the magnetizable particles for magnetic actuated RNA transfer. Therefore the streptavidin coated particles were coupled with newly designed biotinylated hybridization oligonucleotides (HybOligos) hybridizing with the constant region of the mRNA. Four HybOligos hybridizing either to the 5′ end (Hyb5A, Hyb5B) or to the 3′ end (Hyb3A, Hyb3B) of the RNA were designed based on the secondary structure of the RNA template. The biotinylation rate was determined as approximately 95% and was quiet similar for the different HybOligos

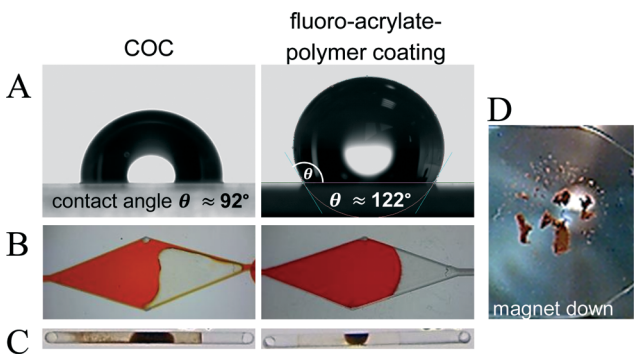

Fig. 4 Manipulation of the wettability of microfluidic structures and their interaction with particles (A–C) and control of particle aggregation (D). (A) Surface modification of microfluidic structures (micro-milled in COC) by coating with a fluoro-acrylate-polymer provides significant advantages: it leads to increased hydrophobicity, (B) it allows repeated pumping of fluids without uncontrolled trapping of air, and (C) the adherence of particles to the microfluidic surface is reduced. (D) Adaption of the surrounding solutions composition modifies zeta potential of the particles and influences particle aggregation. Dispersed particles as shown in Fig. 3B are desired. The zeta potential of the particles in washing solution (0.05 mM Mg^{2+}, pH 7.5) is negative (less than −20mV for HybOligo loaded particles) leading to dispersed particles.

within the limits of experimental fluctuations (data not shown) allowing comparison of HybOligos without a correction factor. The dependence of the mRNA binding capacity on the utilized HybOligo was investigated to identify the best HybOligo. The results were dependent on the time of hybridization: either hybridization of HybOligo and mRNA during TK (Fig. 5B) or hybridization after TK with purified mRNA (Fig. 5A). One reason for this result could be the different conformation of the mRNA while binding. During transcription HybOligos can hybridize to still synthesized and unfolded mRNA. In contrast, following transcription HybOligos hybridize with mRNA with secondary structure. However, the highest binding capacities were always detected for Hyb3A binding outside a hairpin loop of the mRNA and the lowest were detected for Hyb3B binding completely inside a hairpin loop (Fig. 5A and B). Hyb5A and Hyb5B bind partially inside and partially outside a hairpin loop. For binding inside a hairpin loop the complementary sequence on the mRNA competes with the oligonucleotide for the site of hybridization resulting in lower binding efficiencies. During transcription, the site of hybridization for Hyb5A is synthesized first and the complementary sequence on the mRNA afterwards. In contrast, the complementary sequence to the site of hybridization of Hyb5B is synthesized first and afterwards the site of hybridization. This might be a reason for higher hybridization rates for Hyb5A than for Hyb5B during transcription (Fig. 5B). A benefit of the HybOligos binding to the 3′ end is that they would not remove incomplete transcripts still bound to the TK machinery since mRNA is synthesized from the 5′ end to the 3′ end. In conclusion Hyb3A was the most efficient HybOligo.

Neither free HybOligos nor high amounts of functionalized particles (0.8 mg particles in 25 μL TK) inhibited *in vitro* transcription (data not shown) allowing immobilization during TK. Repeated reuse of the particles for immobilization during TK did not inhibit *in vitro* TK (Fig. 5C) indicating that the non-specific binding is low: the particles do not remove the transcription machinery. The reuse of the beads is essential to minimize costs.

Different surface densities of HybOligos on the particles led to different efficiencies for mRNA immobilization. The more HybOligo nucleotides were coupled to the particles, the more mRNA was immobilized in general. However, a maximum concentration of approximately 350 pmol HybOligos per gram particles (Dynabeads® MyOneTM Streptavidin T1) was observed. If the particles were loaded completely with HybOligos, less mRNA is immobilized (data not shown). Similar effects were previously observed.[38–40] To reduce this effect of steric hindrance and to improve the mRNA immobilization efficiency, the HybOligos were modified with oligo$(dT)_{15}$ spacer. The efficiency of immobilization was improved compared to the same HybOligo without the spacer modification (Fig. 5A), and no steric hindrance was observed for complete loading with HybOligos. It was previously observed that the application of spacers can lead to higher hybridization rates.[41–44]

In addition to the immobilization molecules, also the particles were selected from four variants differing in size, charge, iron oxide content and material. None of the particles inhibited *in vitro* transcription or *in vitro* translation in a concentration of approximately 0.1 mg particles per 20 μL reaction volume. "Dynabeads® MyOneTM Streptavidin C1" have a higher iron oxide content and adhere less to the channel surface than other particles. Therefore they were best suited for the transfer process. Moreover, they showed the highest

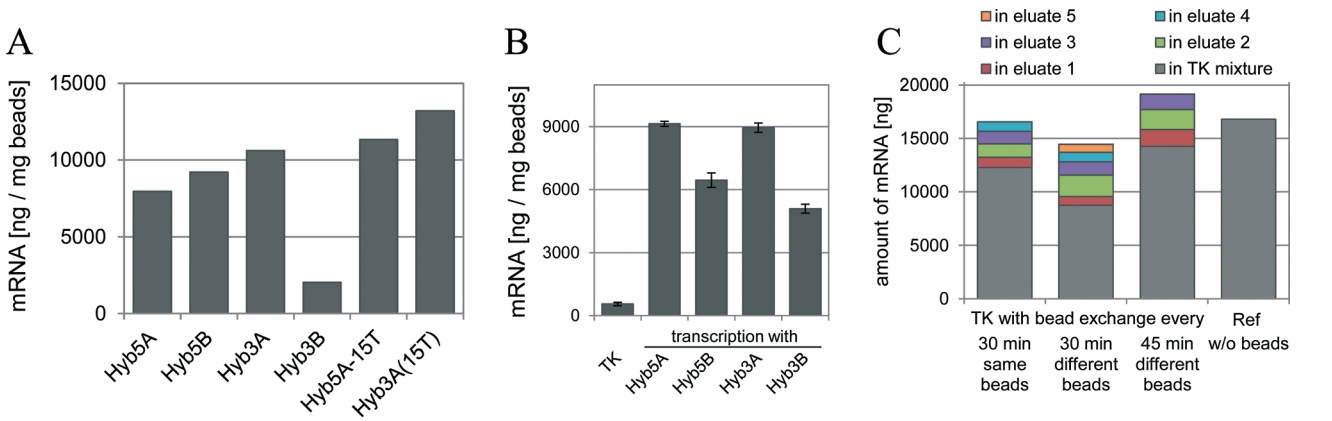

Fig. 5 Dependence of mRNA binding capacity on the used HybOligo and the time of hybridization (A, B) and mRNA immobilization during *in vitro* TK (C). (A–B) Hybridization of the HybOligos with the mRNA was either performed during TK (B) or following TK with purified mRNA (A). Afterwards mRNA was eluted. The bar chart representing the amount of eluted mRNA indicates the efficiency of hybridization. The hybridization at different times leads to different hybridization results. For instance Hyb3B can hybridize better to mRNA which is still synthesized (B) than to already folded mRNA (A). mRNA hybridization to Hyb3A always worked best (A & B). Oligo$(dT)_{15}$ spacer improved immobilization efficiencies (A). Hardly any mRNA was detected in the negative control without a HybOligo. (C) *In vitro* TK of eYFP DNA templates was performed in the presence of 0.15 mg Hyb3A-15T-functionalized particles and as a reference (Ref) without particles (beads). The particles were repeatedly exchanged after 30 min or 45 min. In addition, the same HybOligo-particles were removed, washed, eluted and added again to the TK mixture repeatedly after 30 min. In each case mRNA was produced in similar amounts as in the Ref within the limits of experimental variations. More mRNA is immobilized for longer incubation of the particles in the TK mix. The reuse of the functionalized particles was successful.

binding capacity for HybOligos and mRNA compared to the other particles (data not shown).

Altogether the optimal particle-HybOligo combination for mRNA immobilization is C1 particles with Hyb3A-15T as they showed the highest binding capacities.

Since the immobilization molecules hybridize to the constant region of the mRNA, the immobilization and transfer process is potentially applicable for RNA templates encoding all types of proteins. The process was successfully applied for immobilization and transfer of RNA encoding eYFP, luciferase and Pierisin. Besides the RNA transcribed from PCR templates, RNA transcribed from pIX3.0 plasmids was also successfully immobilized and transferred using the functionalized particles. The use of linearized plasmids for transcription leads to improved RNA immobilization efficiencies compared to circular plasmids. If the polymerase skips its terminator sequence, transcription is terminated by DNA secondary structures or by reaching the terminator sequence again or by reaching the end of linear DNA templates. Therefore, a mixture of normally sized RNA as well as longer RNA is synthesized form circular plasmids. In contrast, only normally sized RNA is synthesized form plasmids linearized a few base pairs downstream of the terminator sequence. Immobilization capacity is inversely related to molecule size which might be due to steric hindrance.

RNA immobilization behavior was characterized for an appropriate design of the parameters in the microfluidic TRITT platform. For instance, kinetics of mRNA immobilization and the influence of the amount of particles and mRNA on mRNA immobilization to the particles were studied. Depending on the current amount of RNA in the TK mixture, approximately 1000–1800 ng mRNA can be immobilized by incubation of 0.15 mg of functionalized particles in TK mixture for 20 minutes. Thus, it is required to repeat the mRNA immobilization and transfer procedure at least 3–6 times to provide sufficient mRNA for a 25 μL TL reaction. Based on these results, the transcription compartment was divided into three chambers. Immobilization of mRNA is independently possible in all these chambers. The beads of the first chamber can be eluted at first and transferred back to the chamber – followed by elution of the beads of the second chamber and the beads of the third chamber. In this manner there is sufficient time for immobilization of mRNA to the individual bead batch prior to its transfer and elution and the entire procedure can be performed sequentially in the three chambers. As a consequence, mRNA transfer is quasi-continuous, and there is no latency due to the immobilization process.

In vitro translation of RNA with and without internal ribosome entry site elements in the presence of free HybOligos

An essential prerequisite for the application of the immobilization and transfer procedure described above is the demonstration of translation of the transferred mRNA. For reasons of simplicity of the design of the microfluidic TRITT platform, it was first evaluated whether the immobilized mRNA can be used directly for translation. It is well known that short oligonucleotides complementary to the mRNA can inhibit TL by physically preventing or inhibiting progression of the translational machinery.[45–47] Various mechanisms of action for translational inhibition are possible, such as for instance CAP initiation inhibition (inhibition of ribosome attachment), inhibition of ribosome transit to the initiation sequence or ribosomal unit joining inhibition.[47] Thus, it was initially investigated whether free HybOligos inhibit *in vitro* translation. *In vitro* translation in the presence of HybOligos (in excess to the RNA) led to lower protein yields compared to a reference translation without oligonucleotides. However, Hyb3B inhibited translation only slightly. One reason might be the low hybridization efficiency of this oligonucleotide (see Fig. 5), and as a consequence the improved ribosome transit or background translation of free mRNA. Another reason might be the binding of Hyb3B inside a double stranded hairpin structure of the RNA, which does not result in a new double strand by hybridization. For clarification, translation was additionally investigated for immobilized mRNA excluding the presence of free mRNA (see below). Hyb5A was obviously the most efficient inhibitor of translation. One reason could be that Hyb5A hybridizes at the 5′ UTR in proximity to the translational initiation codon (17 bp upstream of the initiation codon). Hybridization oligonucleotides with sequences in proximity to the translation initiation codon are frequently very efficient translational inhibitors.[45,47]

To solve the potential problem of inhibition of the promotion of translation (ribosome attachment and transit to initiation sequence) by HybOligo hybridization to the 5′ end of the mRNA, the IRES element KSHV252(+s) and alternatively the IRES element KSHV252(−s) was introduced at the 5′ untranslated region of the RNA. IRES elements were previously applied for CFPS.[48,49] In this study, the introduced IRES element increases the distance to the translation initiation codon and more importantly, IRES elements are alternative ribosomal binding sites and can mediate translation initiation independent of the 5′CAP. Thus attachment and transition of the ribosome can occur downstream of the hybridization sites for Hyb5A and Hyb5B. TL of the RNA harboring an IRES element resulted in decreased eYFP yields compared to TL of RNA without IRES element. However, eYFP synthesis was slightly increased in the presence of free HybOligos – especially in the presence of Hyb5A – compared to TL without HybOligos. This might be explained as follows: the IRES-dependent translation was inhibited in the presence of the CAP. Binding of the HybOligos inhibits the CAP-dependent translation and thereby improves the IRES-dependent translation. IRES-dependent translation was not affected by HybOligo binding. Thus, immobilization of IRES-mRNA without CAPs *via* Hyb5A/5B could allow efficient solid-phase translation.

In vitro translation of eluted RNA or immobilized RNA

For translation of immobilized mRNA, the mRNA-HybOligo-particles were previously washed with a buffer with an ionic

milieu similar to the translation mixture (2.5 mM Mg^{2+}, 125 mM K^{+}) for conditioning and removal of unbound mRNA. The particles with immobilized mRNA were subsequently used for TL. As depicted in Fig. 6 high amounts of (non-functionalized) particles inhibited *in vitro* translation of free mRNA. In contrast, smaller amounts of particles did not inhibit translation. However, the obtained eYFP yield was higher than in the no template control and comparison with TL of immobilized mRNA is possible. The amount of functional eYFP synthesized by TL of immobilized mRNA was in the range of the no template control. Only one exception was observed: the use of Hyb3B-C1 particles resulted in eYFP signal intensities in the range of the references intensities (TL of free mRNA in the presence of non-functionalized particles). This might indicate that translation of mRNA immobilized to Hyb3B is indeed not inhibited by the hybridization of the oligonucleotide. However, the large amount of particles is required for transfer of sufficient mRNA for efficienttranslation, but inhibits translation. Probably another solid support would have sufficient mRNA binding capacities and would therefore allow efficient IRES-mediated translation of immobilized mRNA.

In vitro translation was additionally performed with free mRNA eluted from the particles. Initially mRNA carrying particles were washed with a low-salt washing buffer (50 mM KCl), subsequently the particles were incubated for 2 min at 70 °C in an elution buffer (30 mM HEPES, pH 7.5) for mRNA elution. The resulting eluate was applied for TL. Functional eYFP yields comparable to the range of the reference TL of free mRNA purified with DyeEx columns were reached. Since the eluate from a large amount of particles does not inhibit TL, it can be assumed that no HybOligos were removed from the particles by elution since they would inhibit translation.

Optimization of washing and elution procedure

A washing and elution procedure was implemented in the microfluidic TRITT platform since efficient translation still requires free RNA templates. Washing was performed to remove residuals of the TK mix such as RNA polymerase, non-bound nucleotides and magnesium ions (lower magnesium concentration in TL than in TK) and to down-regulate the ion concentration for improved elution conditions (less stringent conditions than for hybridization). Throughout the entire procedure, it was ensured that the washing step does not remove the mRNA. Furthermore, the washing and elution solution had to be adapted for prevention of aggregation of the particles, since the zeta-potential of the particles is dependent on the surrounding media (compare Fig. 3B and 4D). All washing and elution conditions were adapted for these special requirements.

Repeated washing with 0.05 mM Mg^{2+} solution led to highest efficiencies for the following elution step. Lower cation concentrations did not shield the negative charged

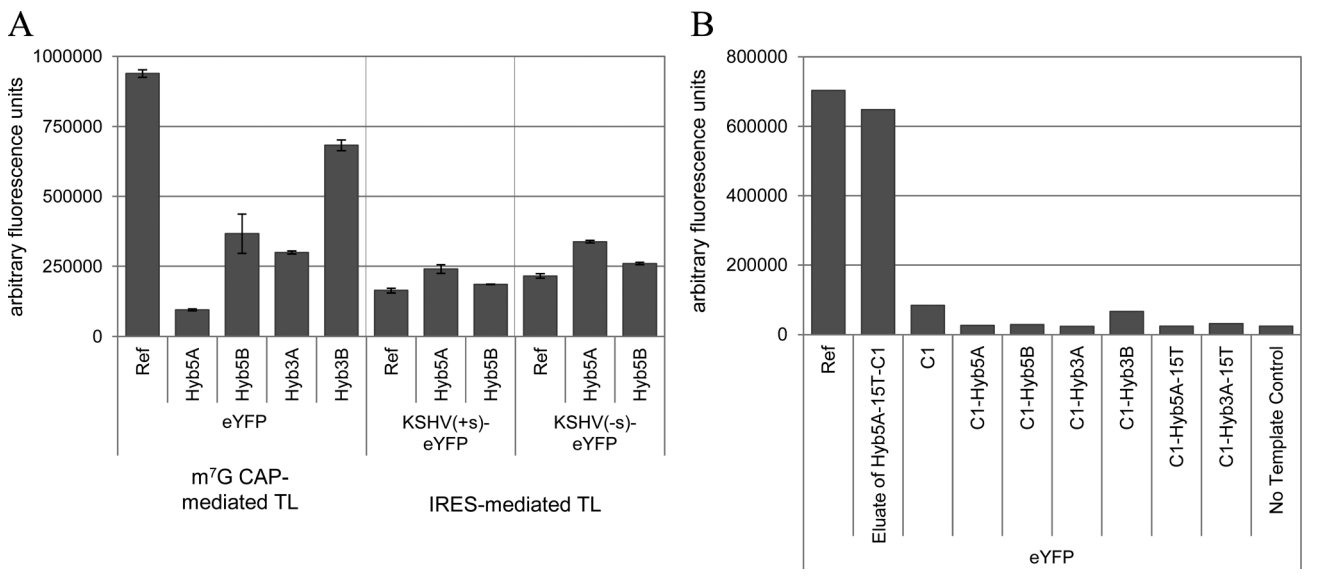

Fig. 6 *In vitro* translation of RNA with and without internal ribosomal entry site (IRES) elements in the presence of free HybOligos (A) and *in vitro* translation of RNA immobilized to or eluted from HybOligo-functionalized particles (B). (A) TL of eYFP-RNA without additional IRES elements was inhibited in the presence of HybOligos. Only slight inhibition of TL was observed in the presence of Hyb3B – the HybOligo binding within a double-stranded hairpin structure and with extremely low hybridization efficiency. The use of mRNA with IRES elements for TL resulted in decreased eYFP synthesis as compared to mRNA without IRES. However, eYFP synthesis was slightly increased in the presence of Hyb5A/5B for TL of mRNA with IRES indicating potential importance of IRES elements for TL of immobilized mRNA. (B) TL with the amount of beads necessary for providing sufficient mRNA (1 mg) led to extremely decreased eYFP synthesis (even for non-functionalized beads). eYFP signal intensities in the range of the no template control were detected for TL of (IRES-) eYFP RNA templates immobilized to HybOligo beads. The exception was the use of Hyb3B-beads, for which the fluorescence was slightly higher. *In vitro* TL of the mRNA eluted from beads led to similar eYFP yields as the Ref TL of DyeEx purified mRNA. Therefore, elution was realized for the on-chip procedure.

phosphates at the nucleic acids strands resulting in strong repulsion forces and dehybridization. Higher cation concentrations led to decreased elution efficiencies in the following elution step since a little washing solution remained on the particle's surface and the cations stabilized the double strands. Elution was most efficient in a separate non-ionic buffer without stabilizing cations and at a temperature above the melting point of the RNA-DNA hybrids (70 °C). In detail, all mRNA theoretically bound to the particles, was eluted by the described elution procedure (Fig. 7B).

The functionalized particles were repeatedly reused for immobilization during *in vitro* TK, resulting in similar quantities for each run of immobilization (Fig. 5C). This indicates that the HybOligos were not removed by the washing and elution procedure. Neither Streptavidin was denatured nor was the streptavidin-biotin interaction broken.

On-chip *in vitro* transcription, immobilization, transfer and elution of eYFP-mRNA

To enable automated CFPS using the novel TRITT mode, the mRNA immobilization and transfer procedure was implemented into a microfluidic device. The microfluidic components required for fluid handling, heat transfer and magnetic actuated particle transfer were developed and combined into a working system.

All materials and components required for the device assembly were previously tested for their biocompatibility within the individual CFPS reaction steps. IR thermography and biological experiments revealed that heating pads with heat spreaders were able to set the desired process temperature homogenously over a large chamber: similar eYFP-mRNA yields were reached for TK in reaction vessels in a thermo cycler and for TK in a compartment of a microfluidic device with a temperature controlled thermal resistor (data not shown). Furthermore, no degradation or hydrolysis of mRNA was observed in the TK mixture in a microfluidic device for more than 19 h of incubation (Fig. 7A), allowing mRNA production and transfer for at least 19 h and indicating a RNase free production of the microfluidic device.

Moreover, the whole procedure, including mRNA immobilization to magnetizable particles during transcription, magnetic actuated particle transfer, particle washing, mRNA elution and mRNA transfer to the translation compartment, was successfully implemented into a microfluidic device: within the limits of experimental fluctuations, the same amount of eYFP-mRNA was immobilized and eluted on-chip and in reaction vessels (Fig. 7B), indicating that all steps were successfully performed and the *de novo* synthesized mRNA did not stick to the channel or tubing surface.

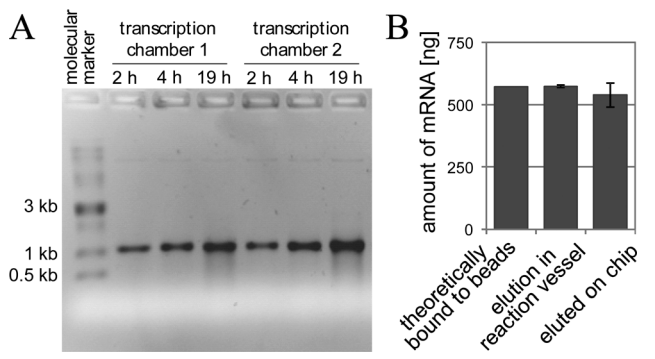

Fig. 7 *In vitro* transcription, RNA-Immobilization, -transfer and -elution in the microfluidic TRITT platform. (A) *In vitro* synthesis of eYFP-mRNA in the TK chambers of the microfluidic device. There is no degradation or hydrolysis of mRNA for more than 19 h of incubation, thus allowing mRNA production and transfer for at least 19 h. (B) eYFP-mRNA was synthesized and immobilized to ≈0.1 mg magnetizable particles in the TK chamber of the TRITT device. Following magnetic actuated particle transfer to the washing chamber, mRNA-carrying particles were washed with 0.5 mM Mg^{2+} solution. Finally, mRNA was removed from the particles by temperature (70 °C) and low salt driven (water) elution in the elution chamber of the TRITT device. As a reference, all steps were performed manually in a reaction vessel. mRNA concentration was determined spectrometrically.

On-chip *in vitro* TK, immobilization, transfer and elution of Pierisin-mRNA and on-chip cell-free synthesis of Pierisin

Expression of cytotoxic proteins is one of the most promising applications of cell-free protein synthesis, since this is hardy feasible using cell-based expression systems. For instance, the coupling of antibodies with apoptosis-inducing proteins is applicable for combatting cancer, and the characterization of toxins is important for the development of tests for food monitoring.[17,50] Another application for CFPS is the incorporation of non-canonical amino acids enabling the production of proteins with new biochemical characteristics.

To demonstrate the applicability in these fields, the microfluidic device was applied for cell-free production of the cytotoxic protein Pierisin (Fig. 8). Thereby, Pierisin was fluorescently labeled by statistical incorporation of the non-canonical amino acid Bodipy-TMR-lysine (boron-dipyrromethene) during *in vitro* TL. Initially, the Pierisin-mRNA was synthesized, immobilized and transferred inside the microfluidic TRITT-platform. Analysis of this mRNA by agarose gel electrophoresis and quantification confirmed intactness and correct size of the Pierisin-mRNA and verified that sufficient mRNA was isolated and transferred for subsequent *in vitro* translation (data not shown). On-chip transcription led to similar Pierisin-RNA yields as compared to transcription in regular reaction vessels. The mRNA isolated using the microfluidic platform was applied for *in vitro* translation. Pierisin was either expressed in a translation chamber of the microfluidic platform or in a normal reaction vessel. In all the cases Pierisin was successfully synthesized: Pierisin-bands appeared at the expected size in the SDS-PAGE gel (Fig. 8A) and the apoptosis-inducing activity was experimentally verified by exposure of HeLa cells to the synthesized proteins (Fig. 8B): Pierisin had a cytotoxic effect and caused morphological changes in HeLa cells. Further, the incorporation of the non-canonical amino acid was proved by fluorescence analysis of the SDS-PAGE gel: similar patterns were detected for

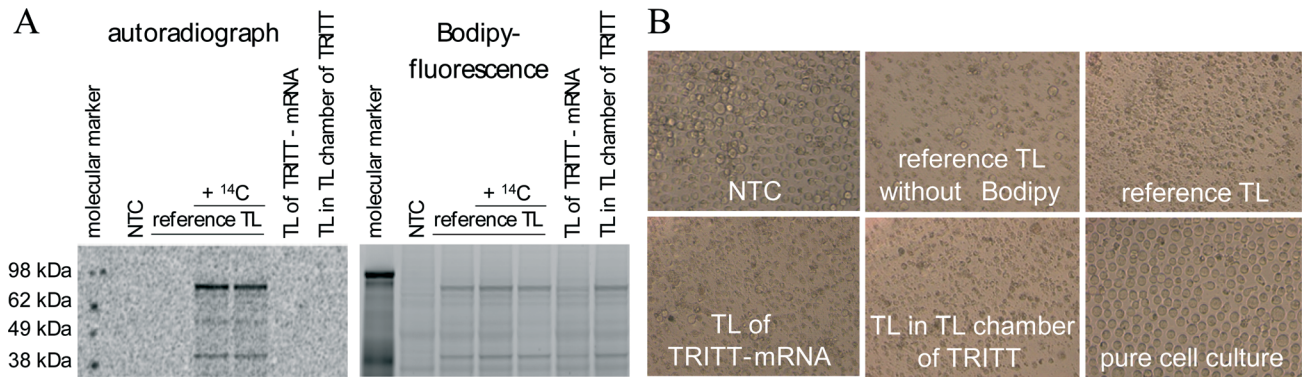

Fig. 8 Cell-free synthesis of the cytotoxic protein Pierisin labeled with the artificial amino acid Bodipy-TMR-lysine using the microfluidic TRITT platform. (A) All the translation reactions were performed in the presence of Bodipy-TMR-lysine for fluorescence labeling. Two references were additionally radioactively labeled with ^{14}C-leucine. Following gel electrophoresis, the labeled synthesized proteins were visualized by autoradiography and fluorescence analysis (excitation: 532 nm, emission: BP 580 nm) using the Typhoon Trio + Imager (GE Healthcare). Although less mRNA was provided for TL of the transferred TRITT-mRNA, Pierisin (97.9 kDa) was successfully expressed using the TRITT-mRNA and in the TL chamber of the microfluidic device. Bodipy labeling was successful and the detected bands in the SDS-PAGE gel are comparable to the bands visualized by ^{14}C labeling. (B) Cytotoxic activity of Pierisin: HeLa cells were cultured to near confluency and 4 μL of the respective translation mixtures were added to 100 μL of cell culture medium. Following 48 h of incubation, the cells were analyzed by microscopy. Cell-free synthesized Pierisin – translated from microfluidic separated mRNA and cell-free synthesized in a normal reaction vessel or in the TL chamber of the TRITT platform – is active and causes morphological changes in HeLa cells. Cell death is not induced by the no template control (NTC).

Bodipy-TMR-lysine labeled and ^{14}C-leucine labeled proteins (Fig. 8A).

All experiments were performed in a semi-automated manner: the fluids flow was induced by the syringe pumps and the magnetic particles were transferred with the magnetic device – both processes were software-controlled using predefined program steps. Modification of the standard program flow was necessary to compensate remaining wetting problems due to changing surface conditions.

Conclusions

A new procedure to immobilize and transfer RNA templates for CFPS was developed and all processes required for automated CFPS, including mRNA immobilization to magnetizable particles during TK, magnetic actuated particle transfer, particle washing, mRNA elution, mRNA transfer to the TL compartment and TL, were successfully implemented into a microfluidic device. mRNA eluted from the particles was successfully used for *in vitro* translation and the particles were reusable for additional steps of mRNA immobilization. The preconditions for automated cell-free protein synthesis in modular microfluidic reactor systems were thereby fulfilled. The developed procedure enables a new reaction mode – called TRITT mode: mRNA is removed from the transcription mixture without inhibition of the transcription reaction and the mRNA can be transferred to the translation compartment and can be efficiently translated while mRNA is synthesized continuously in the transcription compartment. This saves valuable user time as in a coupled system while allowing optimal conditions for TK and TL like in the linked system, combining these advantages. Further integration of dialysis membranes, microelectronics or micro optical sensors and actuators might allow measurement and regulation of relevant reaction parameters for optimal reaction conditions allowing longer reaction times, higher yields and improved amounts of functional proteins. For example dialysis systems yield 1.2 mg protein per mL in 14 h having the limitation of RNA degradation in TL mixture.[30] A combination with the TRITT mode would enable automated feeding of RNA reducing this limitation. Moreover, the TRITT mode facilitates further fields of applications such as transcription of different DNA templates and combination of the generated RNA templates in desired amounts for synthesis of different subunits of a protein in a single TL system.

A broad spectrum of applications of the presented microfluidic TRITT platform was demonstrated: PCR products as well as plasmids were provided as DNA templates, and RNA templates encoding various proteins (eYFP, Luciferase, Pierisin) were synthesized, immobilized and transferred using the TRITT mode method. *In vitro* translation of eYFP and Pierisin and the simultaneous incorporation of non-canonical amino acids were performed in the TL compartment. The applicability to the production of toxic proteins and to incorporation of new biochemical features was thereby confirmed.

In summary, the novel microfluidic TRITT platform enables for the first time CFPS with quasi-continuous mRNA transfer under continuously optimal conditions simultaneously for *in vitro* transcription and translation, to the best of the knowledge of the authors. The realized RNA transfer process on the platform is superior to conventional RNA purification methods since it is simpler to automatize and does not terminate transcription. Moreover, quasi-continuous transfer of synthesized mRNA can overcome problems of CFPS due to RNA hydrolysis and degradation. The ability of

RNA transfer to the translation compartment from the beginning of transcription instead of following TK is time saving, since TL can be started while RNA is still synthesized. Furthermore, the implementation of multiple steps into one microfluidic device provides significant advantages in terms of reduced risk of contamination, less reagent consumption, reduced manpower and costs as well as less process time.

An interesting use case scenario would be the effective analytical- or microscale production of otherwise-difficult-to-express proteins, which could be enabled by the integration of a dialysis TL system into the TRITT platform.

Acknowledgements

This research was funded by the German Federal Ministry for Education and Research (BMBF, No. 0312039 and 0315942), and by Fraunhofer in the scope of the Lighthouse Project "Cell-Free Bioproduction". We also thank Conny Mascher and Robert B. Quast for providing essential compounds for cell-free protein synthesis.

Notes and references

1 M. G. Casteleijn, A. Urtti and S. Sarkhel, Expression without boundaries: Cell-free protein synthesis in pharmaceutical research, *Int. J. Pharm.*, 2013, **440**(1), 39–47.
2 F. Katzen, G. Chang and W. Kudlicki, The past, present and future of cell-free protein synthesis, *Trends Biotechnol.*, 2005, **23**(3), 150–156.
3 E. D. Carlson, R. Gan, C. E. Hodgman and M. C. Jewett, Cell-free protein synthesis: Applications come of age, *Biotechnol. Adv.*, 2012, **30**(5), 1185–1194.
4 J. R. Swartz, Developing cell-free biology for industrial application, *J. Ind. Microbiol. Biotechnol.*, 2006, **33**, 476–485.
5 C. J. Noren, S. J. Anthony-Cahill, M. C. Griffith and P. G. Schultz, A general method for site-specific incorporation of unnatural amino acids into proteins, *Science*, 1989, **244**(4901), 182–188.
6 I. Hirao, T. Ohtsuki, T. Fujiwara, T. Mitsui, T. Yokogawa, T. Okuni, H. Nakayama, K. Takio, T. Yabuki, T. Kigawa, K. Kodama, T. Yokogawa, K. Nishikawa and S. Yokoyama, An unnatural base pair for incorporating amino acid analogs into proteins, *Nat. Biotechnol.*, 2002, **20**(2), 177–182.
7 N. Budisa, Expression of 'tailor-made' proteins via incorporation of synthetic amino acids by using cell-free protein synthesis, in *Cell-free protein expression*, Springer Verlag Berlin, 2003, pp. 89–98.
8 M. Gerrits, J. Strey, I. Claußnitzer, U. von Groll, F. Schäfer, M. Rimmele and W. Stiege, Cell-free synthesis of defined protein conjugates by site-directed cotranslational labeling, in *Cell-free protein expression*, RG Landes Co, Austin, 2007.
9 D. Schwarz, V. Dötsch and F. Bernhard, Production of membrane proteins using cell-free expression systems, *Proteomics*, 2008, **8**, 3933–3946.
10 F. Katzen, J. E. Fletcher, J.-P. Yang, D. Kang, T. C. Peterson, J. A. Cappuccio, C. D. Blanchette, T. Sulchek, B. A. Chromy, P. D. Hoeprich, M. A. Coleman and W. Kudlicki, Insertion of membrane proteins into discoidal membranes using a cell-free protein expression approach, *J. Proteome Res.*, 2008, **7**, 3535–3542.
11 F. Katzen, T. C. Peterson and W. Kudlicki, Membrane protein expression: no cells required, *Trends Biotechnol.*, 2009, **27**, 455–460.
12 D. F. Savage, C. L. Anderson, Y. Robles-Colmenares, Z. E. Newby and R. M. Stroud, Cell-free complements in vivo expression of the E. coli membrane proteome, *Protein Sci.*, 2007, **16**, 966–976.
13 S. Kubick, M. Gerrits, H. Merk, W. Stiege and V. A. Erdmann, In vitro synthesis of posttranslationally modified membrane proteins, in *Current Topics in Membranes*, Elsevier Inc., 2009, vol. 63, pp. 25–49.
14 J. R. Swartz and J. J. Wuu, High yield cell-free production of integral membrane proteins, *Biochim. Biophys. Acta, Biomembr.*, 2008, **1778**(5), 1237–1250.
15 S. F. Fenz, R. Sachse, T. Schmidt and S. Kubick, Cell-free synthesis of membrane proteins: Tailored cell models out of microsomes, *Biochim. Biophys. Acta*, 2014, **1838**, 1382–1388.
16 R. Sachse, S. K. Dondapati, S. F. Fenz, T. Schmidt and S. Kubick, Membrane protein synthesis in cell-free systems: From bio-mimetic systems to bio-membranes, *FEBS Lett.*, 2014, **588**, 2774–2781.
17 J. H. C. Orth, B. Schorch, S. Boundy, R. Ffrench-Constant, S. Kubick and K. Aktories, Cell-free synthesis and characterizationof a novel cytotoxic pierisin-like protein from the cabbage butterfly Pieris rapae, *Toxicon*, 2011, **57**, 199–207.
18 S. Bechlars, D. A. Wüstenhagen, K. Drägert, R. Dieckmann, E. Strauch and S. Kubick, Cell-free synthesis of functional thermostable direct hemolysins of Vibrio parahaemolyticus, *Toxicon*, 2013, **76**, 132–142.
19 G. Kanter, J. Yang, A. Voloshin, S. Levy, J. R. Swartz and R. Levy, Cell-free production of scFv fusion proteins: an efficient approach for personalized lymphoma vaccines, *Blood*, 2007, **109**, 3393–3399.
20 J. Yang, G. Kanter, A. Voloshin, N. Michel-Reydelle, H. Velkeen, R. Levy and J. R. Swartz, Rapid expression of vaccine proteins for B-cell lymphoma in a cell-free system, *Biotechnol. Bioeng.*, 2005, **89**, 503–511.
21 L. A. Ryabova, D. Desplancq, A. S. Spirin and A. Pluckthun, Functional antibody production using cell-free translation: Effects of protein disulfide isomerase and chaperones, *Nat. Biotechnol.*, 1997, **15**(1), 79–84.
22 M. Stech, M. Hust, C. Schulze, S. Dübel and S. Kubick, Cell-free eukaryotic systems for the production, engineering, and modification of scFv antibody fragments, *Eng. Life Sci.*, 2014, **14**, 387–398.
23 M. Stech, H. Merk, J. A. Schenk, W. F. M. Stöcklei, D. A. Wüstenhagen, B. Micheel, C. Duschl, F. F. Bier and S. Kubick, Production of functional antibody fragments in a vesicle-based eukaryotic cell-free translation system, *J. Biotechnol.*, 2012, **164**(2), 220–231.

24 A. D. Griffiths and D. Tawfik, Directed evolution of an extremely fast phosphotriesterase by in vitro compartmentalization, *EMBO J.*, 2003, **22**(1), 24–35.
25 N. Goshima, Y. Kawamura, A. Fukumoto, A. Miura, R. Honma, R. Satoh, A. Wakamatsu, J. Yamamoto, K. Kimura, T. Nishikawa and T. Andoh, *et al.*, Human protein factory for converting the transcriptome into an in vitro-expressed proteome, *Nat. Methods*, 2008, **5**, 1011–1017.
26 A. K. Broedel and S. Kubick, Developing cell-free protein synthesis systems: a focus on mammalian cells, *Pharm. Bioprocess.*, 2014, **2**(4), 339–348.
27 M. Stech, A. K. Brödel, R. B. Quast, R. Sachse and S. Kubick, Cell-Free Systems: Functional Modules for Synthetic and Chemical Biology, *Adv. Biochem. Eng./Biotechnol.*, 2013, **137**, 67–102.
28 D.-M. Kim and J. R. Swartz, Regeneration of adenosine triphosphate from glycolytic intermediates for cell-free protein synthesis, *Biotechnol. Bioeng.*, 2001, **74**(4), 309–316.
29 A. S. Spirin, V. I. Baranov, L. A. Ryabova, S. Y. Ovodov and Y. B. Alakhov, A continuous cell-free translation system capable of producing polypeptides in high yield, *Science*, 1988, **242**(4882), 1162–1164.
30 D.-M. Kim and C.-Y. Choi, A Semicontinuous Prokaryotic Coupled Transcription/Translation System Using a Dialysis Membrane, *Biotechnol. Prog.*, 1996, **12**(5), 645–649.
31 G. Grandi, V. A. Shirokov, A. Kommer, V. A. Kolb and A. S. Spirin, *Continuous-exchange protein-synthesizing systems, In vitro transcription and translation protocols*, Humana Press, 2007, pp. 19–55.
32 M. Stech, R. B. Quast, R. Sachse, C. Schulze, D. A. Wüstenhagen and S. Kubick, A Continuous-Exchange Cell-Free Protein Synthesis System Based on Extracts from Cultured Insect Cells, *PLoS One*, 2014, **9**(5), 1–12.
33 M. Biyani, Y. Husimi and N. Nemoto, Solid-phase translation and RNA–protein fusion: a novel approach for folding quality control and direct immobilization of proteins using anchored mRNA, *Nucleic Acids Res.*, 2006, **34**(20), e140.
34 E. Kobatake, A. Ebisawa, O. Asaka, Y. Yanagida, Y. Ikariyama and M. Aizawa, Stabilization and Translation of Immobilized mRNA on Latex Beads for Cell-Free Protein Synthesis System, *Appl. Biochem. Biotechnol.*, 1999, **76**, 217–227.
35 D. E. Lanar and K. Kain, Expression-PCR (E-PCR): overview and applications, *Genome Res.*, 1994, 92–96.
36 R. Sachse, D. A. Wüstenhagen, M. Samalíková, M. Gerrits, F. F. Bier and S. Kubick, Synthesis of membrane proteins in eukaryotic, *Life Sci.*, 2013, **13**(1), 39–48.
37 M. González, L. A. Bagatolli, I. Echabe, J. L. R. Arrondo, C. E. Argaraña, C. R. Cantor and G. D. Fidelio, Interaction of Biotin with Streptavidin THERMOSTABILITY AND CONFORMATIONAL CHANGES UPON BINDING, *J. Biol. Chem.*, 1997, **272**(17), 11288–11294.
38 P. W. Steven, M. R. Henry and D. M. Kelso, DNA hybridization on microparticles: determining capture-probe density and equilibrium dissociation constants, *Nucleic Acids Res.*, 1999, **27**, 1719–1727.
39 A. W. Peterson, R. J. Heaton and R. M. Georgiadis, The effect of surface probe density on DNA hybridization, *Nucleic Acids Res.*, 2001, **29**, 5163–5168.
40 J. H. Watterson, P. A. E. Piunno, C. C. Wust and U. J. Krull, Effects of oligonucleotide immobilization density on selectivity of quantitative transduction of hybridization of immobilized DNA, *Langmuir*, 2001, **16**, 601–608.
41 M. S. Shchepinov, S. C. Case-Green and E. M. Southern, Steric factors influencing the hybridisation of nucleic acids to oligonucleotide arrays, *Nucleic Acids Res.*, 1997, **25**(6), 1155–1161.
42 U. Maskos and E. M. Southern, Oligonukleotide hybridisations on glass supports : a novel linker for oligonucleotide synthesis and hybridisation properties of oligonucleotides synthesised in situ, *Nucleic Acids Res.*, 1992, **20**(7), 1679–1684.
43 B. Joos, H. Kuster and R. Cone, Covalent attachment of hybridizable oligonucleotides to glass supports, *Anal. Biochem.*, 1997, **247**, 96–101.
44 A. Halperin, A. Buhot and E. B. Zhulina, Hybridization at a Surface: The Role of Spacers in DNA Microarrays, *Langmuir*, 2006, **2**(26), 11290–11304.
45 J. J. Toulmé, H. M. Krisch, N. Loreau, N. T. Thuong and C. Hélène, Specific inhibition of mRNA translation by complementary oligonucleotides covalently linked to intercalating agents, *Biochemistry*, 1986, **83**, 1227–1231.
46 K. M. Lee, S. Y. Lee, S. S. Suh and B. L. Lee, Antisense DNA and RNA Oligonucleotides Inhibited Translation of Tabacco Mosaic Virus (TMV) RNA in vitro, *Korean J. Biochem.*, 1992, **25**(2), 120–127.
47 N. Dias and C. A. Stein, Antisense Oligonucleotides: Basic Concepts and Mechanisms, *Mol. Cancer Ther.*, 2002, **1**, 347–355.
48 A. K. Brödel, A. Sonnabend and S. Kubick, Cell-Free Protein Expression Based on Extracts From CHO Cells, *Biotechnol. Bioeng.*, 2013, **111**(1), 25–36.
49 A. K. Broedel, A. Sonnabend, L. O. Roberts, M. Stech, D. A. Wüstenhagen and S. Kubick, IRES-Mediated Translation of Membrane Proteins and Glycoproteins in Eukaryotic Cell-Free Systems, *PLoS One*, 2013, **8**(12), 1–11.
50 S. Kubick, Zellfreie Proteinsynthese – Möglichkeiten der Darstellung zytotoxischer Proteine, *Labor&more*, 2012, vol. 3.12, pp. 66–70.